ACS APPLIED MATERIALS & INTERFACES

Research Article

www.acsami.org

Organic Silicone Sol–Gel Polymer as a Noncovalent Carrier of Receptor Proteins for Label-Free Optical Biosensor Application

Jun Ren,[†] Linghua Wang,[‡,§] Xiuyou Han,[‡] Jianfang Cheng,[‡] Huanlin Lv,[‡] Jinyan Wang,[⊥] Xigao Jian,[⊥] Mingshan Zhao,*[,‡] and Lingyun Jia*[,†]

[†]School of Life Science and Biotechnology and [‡]School of Physics and Optoelectronic Engineering, Dalian University of Technology, No. 2 Linggong Road, Dalian 116023, P. R. China

[⊥]Department of Polymer Science and Materials, Dalian University of Technology, Dalian 116012, P. R. China

[§]Photonics Research Group (INTEC), Ghent University–IMEC, Ghent, B-9000, Belgium

Supporting Information

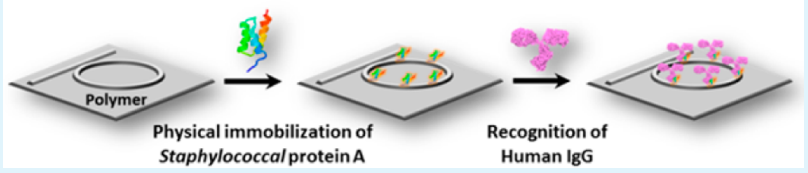

ABSTRACT: Optical biosensing techniques have become of key importance for label-free monitoring of biomolecular interactions in the current proteomics era. Together with an increasing emphasis on high-throughput applications in functional proteomics and drug discovery, there has been demand for facile and generally applicable methods for the immobilization of a wide range of receptor proteins. Here, we developed a polymer platform for microring resonator biosensors, which allows the immobilization of receptor proteins on the surface of waveguide directly without any additional modification. A sol–gel process based on a mixture of three precursors was employed to prepare a liquid hybrid polysiloxane, which was photopatternable for the photocuring process and UV imprint. Waveguide films were prepared on silicon substrates by spin coating and characterized by atomic force microscopy for roughness, and protein adsorption. The results showed that the surface of the polymer film was smooth (rms = 0.658 nm), and exhibited a moderate hydrophobicity with the water contact angle of 97°. Such a hydrophobic extent could provide a necessary binding strength for stable immobilization of proteins on the material surface in various sensing conditions. Biological activity of the immobilized *Staphylococcal* protein A and its corresponding biosensing performance were demonstrated by its specific recognition of human Immunoglobulin G. This study showed the potential of preparing dense, homogeneous, specific, and stable biosensing surfaces by immobilizing receptor proteins on polymer-based optical devices through the direct physical adsorption method. We expect that such polymer waveguide could be of special interest in developing low-cost and robust optical biosensing platform for multidimensional arrays.

KEYWORDS: *optical biosensor, microring resonators, sol–gel polymer, surface modification, protein immobilization, physical adsorption*

1. INTRODUCTION

Label-free monitoring of biomolecular interactions has become of high importance for the current proteomics era.[1] Unlike conventional label-based detection methods that rely on labels (commonly, fluorescent dyes, radioactive molecules or nanoparticles) to report signals, label-free biosensing enable the translation of a binding event into a quantifiable signal of the corresponding sensor in a direct manner, thus achieve a real-time detection. Therefore, label-free biosensors are especially suitable for kinetic interaction studies, on-site monitoring and high-throughput applications, and have emerging applications in functional proteomics[2] and drug discovery.[3]

Optical microring resonator biosensors have gained increasing attention due to its high sensitivity and potential for integration in multidimensional arrays.[4,5] Unlike commonly used surface plasmon resonances (SPR)-based sensing platform, the detection mechanism of this type of biosensors relies on the resonant effect of optical cavities.[4] Briefly, a binding event in the near vicinity of an microring waveguide will change the local refractive index, which results in a change in the effective refractive index of the optical mode and hence in a resonance wavelength shift. This direct signal is proportional to the number of binding events, thus providing a quantitative measure for the amount of the targeted molecules present on the sensor surface (see Figure S1 in the Supporting Information). The increased photon lifetime in an optical cavity results in a sharp resonant peak, enabling the detection of ultrasmall changes of the resonance wavelength.[5] The feasibility of using microring resonators for the label-free detection of various biomolecules and cells, including proteins, oligonucleo-

Received: October 23, 2012
Accepted: December 21, 2012
Published: December 21, 2012

tides, and bacteria, has been demonstrated previously.[6−10] Structural simplicity of microring resonator provides this type of biosensors with two notable properties. First, the response of optical cavities does not decrease with decreasing sensing area, thus tens of sensors can be placed on a square millimeter without loss of sensitivity, with which microarray chips can be developed for high-throughput applications. Bailey and co-workers[7,8] reported a multiplexed platform equipped with 32-element photonic microring resonators arrays, which allowed a 5 min analysis of a variety of T cell cytokine secretion. Second, optical microring sensors can be fabricated from a variety of material systems,[11,12] such as silica-on-silicon, polymers, silicon-on-insulator (SOI), and do not need additional coating of gold lay, which is indispensable for SPR and quartz crystal microbalances (QCM) biosensors. The flexibility in material platform provides a relatively large freedom for the design of biosensors, toward better sensing performance and more versatile applications.

Our designs were orientated toward the development of a low-cost, easy to fabricate, easy to use and robust optical biosensor. A facile and generally applicable method for the immobilization of receptor proteins is an important consideration for both the fabrication and the subsequent use of the sensor chips. For current silicon-based platform of optical waveguide, covalent method is typically utilized, for which a modification process with multistep reactions are usually necessary, normally including surface activation, PEG-modification, receptor molecule coupling and blocking.[13] Other strategies include self-assembled monolayers (SAM) using organophosphonate[14] and aniline-catalyzed coupling reaction between aldehyde and hydrazine.[15] For these methods, the multistep reactions make it labor- and cost-intensive to fabricate sensor chips, especially for microarray application. In addition, the modification process refers to a range of organic reagents and complex treatments that might alter the surface properties of the optical devices. Therefore, a straightforward and cost-effective process for protein immobilization is more attractive. It is desired to explore the potential of polymer optical waveguide that could facilitate the protein coupling process through direct physical adsorption.

Noncovalent immobilization of proteins on a solid phase has been intensively studied for its important role in many different fields,[16−19] including biomedical, biofouling, and bioreactors. The major advantage of this immobilization strategy is its simplicity, with minimal manipulation for mostly high immobilization level. Proteins will interact well with a hydrophobic carrier via van der Waals forces and entropy changes, and also can be immobilized on hydrophilic carriers via hydrogen bonds and ionic interactions.[16] Ideally, the methods that are developed should enable the capture of proteins to generate homogeneous, stable, and high-density protein surfaces with the retention of good protein function. Although there existing some concerns about the unfolding and leaching of adsorbed proteins during a sensing experiment, there are still several studies suggesting that stable and specific immobilization of proteins can be readily achieved, especially for some hydrophobic carriers.[20,21] Interaction force and topographies are two key characteristics of material surface that govern its protein binding performance.[20] To date, several material platforms have been well-developed as protein carrier for bioanalysis or enzyme immobilization applications, including PMMA,[22,23] chitosan,[24] polypropylene[25] and polystyrene.[26] However, to the best of our knowledge, no polymer material has been reported that can satisfy the requirements of both bioanalysis and optical waveguide devices.

This study presents a sol−gel material system for the fabrication of optical devices, which can play the roles as both optical transducer and carrier for receptor proteins, without any physical or chemical modification. Hybrid polysiloxane polymer offers high structural flexibilities by different combinations of the monomers, and accurate control of the material's optical and physical properties can be well obtained.[27] In the present study, a sol−gel system with three precursors, phenyl trimethoxysilane (PTMS), methyl trimethoxysilane (MTMS) and 3-(methacryloxy) propyl trimethoxysilane (MAPTMS), were employed. A Transparent liquid polysiloxane (solvent-free) polymer with moderate hydrophobicity was synthesized initially. Waveguide devices were then fabricated through a process including spin-coating, UV-based soft imprinting and heat condensation. Waveguide films were characterized by X-ray photoelectron spectroscopy (XPS), atomic force microscopy (AFM) to obtain detailed information of their surface properties. We mainly focused on characterizing the protein immobilization performance of the current polymer platform. Finally, this biosensing platform was successfully used to detect the interaction between the immobilized *Staphylococcal* protein A and human Immunoglobulin G, demonstrating its utility in optical biosensing.

2. MATERIALS AND METHODS

2.1. Materials. Phenyl trimethoxysilane (PTMS), methyl trimethoxysilane (MTMS), 3-(methacryloxy) propyl trimethoxysilane (MAPTMS), and other reagents were purchased from Sigma-Aldrich, TCI, and Alfa Aesar and used as received unless otherwise stated. Deionized (DI) water was obtained from a Milli-Q ultrapure water purification system (Millipore, Billerica, MA).

2.2. Preparation of Silicone Sol−Gel Polymer. Following the optimized reaction process previously reported,[28] three precusors, MAPTMS, MTMS, and PTMS, with the molar ratio of 10:75:15 were mixed with 0.1 M HCl, and stirred at 25 °C for 2 h. The product was dissolved in ether and washed with deionized water until neutral, and further went through vacuum drying at 40 °C to remove the remaining solvent. Silicon substrates were coated with polymer film through a spin-coating process. A native oxidized surface was used, on which the sol−gel product was added together with 0.8 wt % photoinitiator PI-184. After treatment in a spin coater, the deposit layer was exposed to UV light (25 mW/cm^2) for 120 s, and then baked at 180 °C for 2 h to achieve condensation.

2.3. Protein Coating. To clean the surface, we immersed silicon and polymer slides in a 5% Tween-20 solution for 20 min, sonicated in DI water for 10 min, and rinsed thoroughly with DI water twice. After this, the slides were dried under a stream of nitrogen. The cleaned slides were further used for protein coating. Bovine serum albumin (BSA), human Immunoglobulin G (IgG) and lysozyme (Lys) were chosed as model proteins, and labeled with fluorescein isothiocyanate (FITC) for fluorescence analysis (see the Supporting Information for details). For protein adsorption studies, BSA-FITC, IgG-FITC and Lys-FITC solutions were prepared in PBS (0.01 M, pH7.4, containing 0.154 M NaCl) at a concentration of 0.5 mg/mL. Adsorption was performed for 1 h at 37 °C, and another 12 h at 4 °C. Upon completion of adsorption, the slides were thoroughly washed with PBS (0.01 M, pH7.4, containing 0.154 M NaCl) and DI water separately, and the slides were dried with nitrogen for subsequent analysis.

2.4. Determination of Protein Adsorption on PA-Coated Polymer Slides. PA-coated polymer slides were prepared with the same approach as above, except that Protein A was employed as coating molecules. The coated polymer slides were immersed in three different solutions, containing BSA-FITC, IgG-FITC and Lys-FITC respectively to evaluate its adsorption selectivity toward IgG. The solutions of proteins in PBS were prepared at a concentration of 0.5

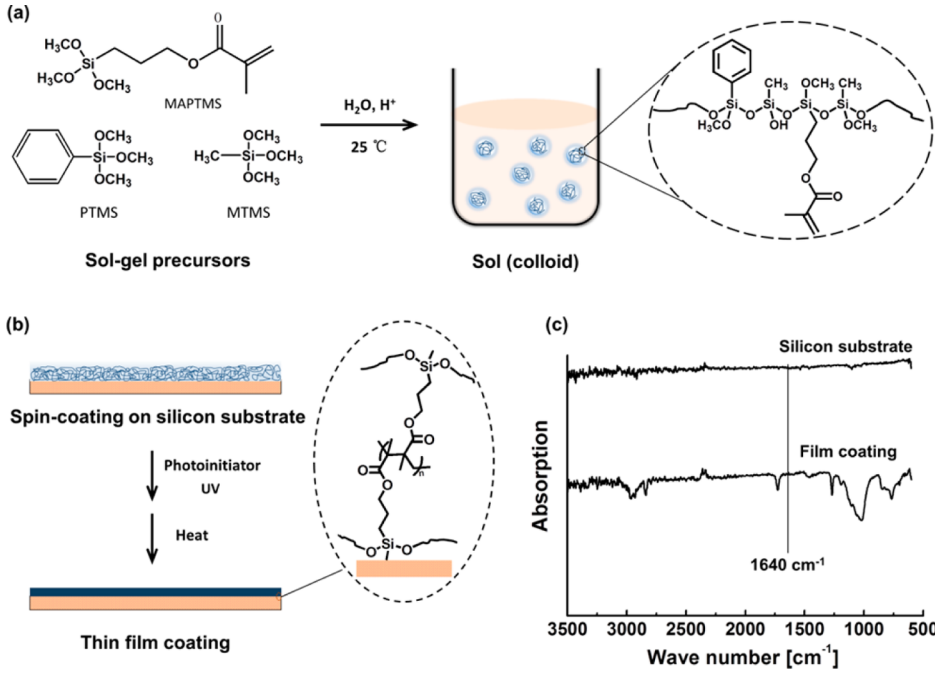

Figure 1. Fabrication of sol–gel modified silicon substrate: (a) acid-catalyzed reaction to prepare silicon sol; (b) condensation of thin film on silicon substrate; (c) FT-IR spectra of the sol–gel film cured on silicon substrate.

mg/mL, and each solution was incubated with a PA-coated polymer slide for 10 min at room temperature. The slide was then rinsed carefully with PBS and dried with nitrogen for the detection of fluorescence signals. BSA-coated polymers were also prepared and tested for comparison.

2.5. Detection of Fluorescence Signals. Fluorescence images were collected using an Olympus IX71 microscope equipped with a 100 W mercury lamp. All pictures were taken under identical lamp illumination and charge-coupled device (CCD) exposure conditions: magnification 100×, exposure time 1/7 s. The fluorescence micrographs were quantitatively analyzed using the software of ImageJ. Each micrograph was transformed into a gray scale image, and its fluorescence intensity was defined as an average gray scale value of a given area based on the statistics of every pixel within the area. The results were expressed in a form of (255 − average gray scale)/255. We assume that the fluorescence intensity is proportional to the amount of adsorbed proteins, but fluorescence intensity could not reflect the amount of protein directly when comparing different proteins because of varying FITC coupling amount on each kind of protein. The term of normalized intensity was defined to reflect the amount of adsorbed proteins directly by considering F/P mass ratio (the ratio of masses of FITC to masses of protein in the conjugate) of each protein and the effect of fluorescence background of slide material. F/P mass ratio and F/P molar ratio of the three proteins are shown in Table S1 of the Supporting Information.

2.6. Sensor Fabrication and Measurement. The microring resonator based optical waveguide biosensor is fabricated by UV-soft imprint technique with a polydimethylsiloxane (PDMS) mold. A 2 μm-thick layer of polymer was spin-coated on the Si/SiO_2 substrate. After that, the prepared soft PDMS mold with the waveguide patterns on it is used to imprint this layer. Around 3 min of UV illumination with an intensity of 30 mW/cm^2 in nitrogen atmosphere is used to cure the waveguide core layer. The waveguide patterns can be shaped with good conformity to those on the mold. After detaching the waveguide from the mold, post baking at 180 °C for 2 h and 200 °C for another 2 h allows full polymerization of the waveguide core layer. The radius of the microring is set to be 700 μm. The gap and coupling length between the straight waveguide and the racetrack microring resonator are designed to be 1 and 70 μmm respectively. After the surface functionalization of the polymer ring resonator with receptor proteins, the chip was assembled with the microfluidic channel and mounted onto a measurement system.

2.7. Detection of Human IgG by Protein A-Functionalized Polymer Microring Resonators. A typical binding experiment was preceded by flowing DI water over the surface to stabilize the sensor response. PBS (0.01 M, pH 7.4) and the sample of human IgG (solution in 0.01 M PBS, pH 7.4) were pumped into the fluidics channel consecutively at the speed of 10 μL/min, followed by another run of PBS to examine dissociation. IgG samples with the concentration of 50 μg/mL and 5 μg/mL were applied separately; a solution of BSA (50 μg/mL in 0.01 M PBS, pH 7.4) was used as the control. The resonant peak position was recorded as a function of the time during the process.

2.8. Water Contact Angle Measurements. Static water contact angles were measured at room temperature using the sessile drop method and image analysis of the drop profile. The instrument, using a CCD camera and an image analysis processor, was purchased from Dataphysics Research, Inc. (USA). The water (Milli-Q) droplet volume was 1 μL, and the contact angle was measured 5 s after the drop was deposited on the sample. For each sample, the reported value is the average of the results obtained on three droplets.

2.9. Surface Characteration. *AFM Analysis.* AFM measurements were performed in air using a Nano Scope IIIa ADC5 (Veeco Metrology Group, USA). If not explicitly mentioned, the tapping mode was used and the applied force was always minimized, so as not to deform the soft protein layers.

Fourier Transfer Infrared (FTIR) Analysis. Reflectance FTIR spectra were collected on an Equinox 55 ATR-FTIR spectrometer (Bruker Instruments, Germany) using a resolution of 8 cm^{-1} and a total of 1000 scans per sample. For all reflectance measurements of the functionalized silicon surfaces, the initially cleaned substrates were used as a reference.

XPS Analysis. XPS measurements were performed with a ESCALAB 210 electron spectrometer (VG Scientific Ltd., UK) using Mg KR radiation under a vacuum of 2 × 10^{-8} Pa.

3. RESULTS AND DISCUSSION

3.1. Synthesis of Organic Silicone sol–Gel Polymer. A sol–gel process was employed to prepare polysiloxane-based polymer at room temperature. The reaction is illustrated in

dx.doi.org/10.1021/am3024355 | ACS Appl. Mater. Interfaces 2013, 5, 386–394

Figure 1. The polymer platform was designed by considering its combined roles of both optical waveguide and noncovalent carrier of proteins. First, the material should have a low optical loss to ensure good optical waveguides; second, the surface of the film should have moderate extent of hydrophobicity for stable attachment of receptor proteins; third, certain physical properties (e.g., viscosity and thermal stability) of the polymer material are needed to facilitate the film formation and the fabrication of optical waveguide devices. To meet these demands, we chose and optimized a reaction system with three precursors (Figure 1a), PTMS, MTMS, and MAPTMS.[28]

Transparent liquid polysiloxane (solvent-free) polymer was obtained after the hydrolysis of the three precursors. The viscosity and refractive index of the product are determined mainly by the molar ratio of PTMS component to MTMS component in the hybrid system; increasing the percentage of MTMS will lead to a corresponding decreasing in viscosity and refractive index of the product. A relatively low viscosity is important to facilitate the following spin coating process. However, phenyl groups that were introduced by the component of PTMS had proven effective in increasing both the refractive index and surficial hydrophobicity of the polymer film.[28,29] Thus the ratio of PTMS component is an important parameter in controlling the film's optical property, as well as its ability to bind proteins. In the optimized protocol that employed MTMS at a molar ratio of 75% and PTMS of 15%, the viscosity of the polymer product was 54 mPa/s, applicable for a good control of film thickness (from 1 to 6 μm) during the spin coating process. The refractive index of the resulting polymer was measured as 1.45 at the telecommunication wavelengths (1310 and 1550 nm).

Allyl groups could be cross-linked by UV irradiation. Therefore, the addition of MAPTMS component provided the resultant polysiloxane polymer with UV curable property, and waveguide devices could thus be fabricated through UV-based soft imprint technique. The results showed that the presence of MAPTMS at a molar ratio of 10% could make the sol–gel polymer curing within 3 min under UV light (25 mW/cm^2). Figure 1c shows the infrared spectra of the sol–gel film cured on silicon substrate. C═C stretching vibrational mode resulting from the methacrylic groups appears at 1640 cm^{-1}. In the sample spectra, It can be observed that there is no C═C stretching vibrational mode after UV curing, indicating that the complete cross-linking reaction between the oligomers of polysiloxane during UV curing has been fulfilled for highly compacted organic–inorganic hybrid materials.

The patterned polymer lay was further solidified through a step of heat treatment to form stable waveguide. The condensation of SiOH residues could be carried out both within the film and at the interface with the Supporting Information (Figure 1b). It has been noted that the presence of SiOH residues would lead to significant increase in optical loss, thus heat treatment in high temperature was employed to guarantee the complete condensation of SiOH residues. It can be observed in Figure 1c that the cured sol–gel film has no absorption at 3342–3420 cm^{-1}, a band that corresponds to OH stretching of SiOH, CH_3OH, and H_2O. This means that almost all hydrolyzed species were condensed well. The resulting material has proved to have a good optical property with a relatively low optical loss (<0.3 dB/cm at 1310 nm, <0.9 dB/cm at 1550 nm). This polymer has also been found to have a high thermal stability (1% Td is above 300 °C in air and 340 °C in nitrogen) to meet the requirement for waveguide fabrication. With the current material platform, microring resonators with Q factor as high as 5×10^4 has been produced, which is among the highest values reported so far for polymer based microring resonators.

3.2. Surface Characterization. Surface characteristics of the polymer waveguide, in terms of surface roughness, hydrophobicity and protein attachment ability, were assessed through AFM, XPS analysis and static water contact angle measurements. Figure 2 illustrates the surface morphology for

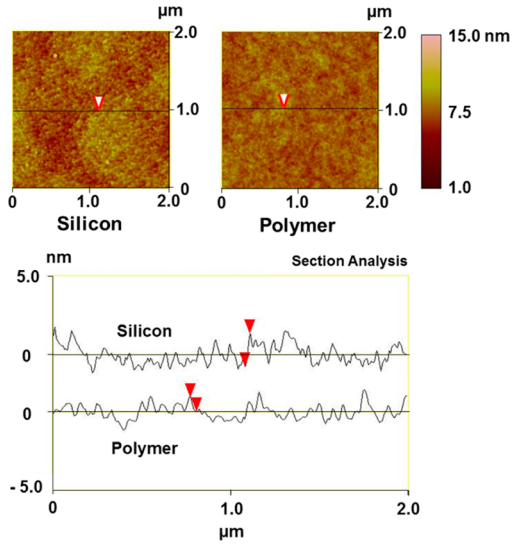

Figure 2. AFM topographical image of uncoated and sol–gel polymer-coated silicon substrate.

the polymer-coated and blank silicon substrates obtained by AFM. Even though the Root-mean-square (Rms) roughness of the blank silicon surface was relatively small (0.67 ± 0.14 nm), no significant change in surface roughness (rms = 0.658 ± 0.20 nm, n = 3) and surface morphology was observed after surface coating with sol–gel polymer. AFM measurements did not show apparent evidence for major heterogeneities in the film. A homogeneous polymer layer is therefore assumed to be present, which is crucial to ensure a good optical property for waveguide materials.[5]

XPS measurement was performed on freshly cleaned silicon substrate as well as sol–gel polymer- and protein-coated surface (Figure 3). Carbon (C 1s), oxygen (O 1s), nitrogen (N 1s), and silicon (Si 2p) spectra were recorded and evaluated quantitatively. Freshly cleaned silicon substrate with a native oxidized surface showed representative signals of Si 2p (103.2 eV), O 1s (532.6 eV), and also weak signals related to carbon containing species (285.2 eV), which maybe due to minor adventitious contamination. Surface-coating of waveguide polymer onto silicon substrate (Figure 3a, middle) resulted in a decrease in the Si signal while an increase in the C 1s (287.3 eV) signal compared to the bare silicon substrate, demonstrating successful modification by sol–gel polymer. As a sensitive surface analytical tool, XPS has been used for detailed studies of the protein interfacial chemistry on surfaces.[30] After BSA adsorption onto the surface of polymer layer, a distinct N 1s (399.3 eV) peak was observed, whereas no N 1s peak was detected on original polymer surface. This result confirms the binding of protein on polymer surface under physiological conditions (Figure 3b). Surface chemical composition calculated from high-resolution XPS spectra are shown in Table 1.

dx.doi.org/10.1021/am3024355 | ACS Appl. Mater. Interfaces 2013, 5, 386–394

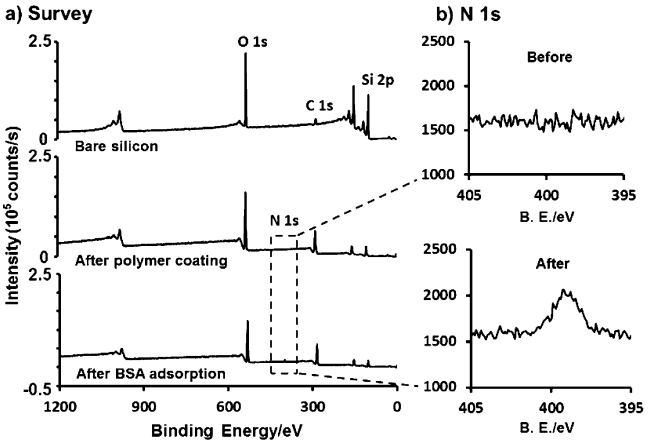

Figure 3. XPS characterization of sol–gel polymer- and protein-coated substrate (a) XPS characterization of bare, sol–gel polymer-modified, and further BSA-coated silicon substrate. (b) High-resolution N 1s region of polymer-modified surface before and after adsorption of the protein.

Table 1. XPS Data for Surface Elemental Composition

sample	% Si	% O	% C	% N
silicon substrate	60.4	31.0	8.6	
sol–gel polymer	18.9	35.7	45.4	
BSA-coated polymer	17.7	32.4	48.2	1.7

The Si content decreased from 60.4% to 18.9% after modification with sol–gel polymer, whereas significant increase in C (from 8.6% to 45.4%) content was observed after coating silicon substrate with sol–gel polymer. After protein immobilization, Si, C, and O content changed only slightly compared to polymer-coated substrates. Measurable N signal was detected only on the protein-immobilized substrates.

Consistent with the XPS observations, the changes in static water contact angle also confirmed the sequential formation of polymer coating and protein binding. Increased surface hydrophobicity was observed after polymer coating (from 65.5 ± 1.2° to 96.8 ± 0.4°), which decreased dramatically to 58.55 ± 2.9° after BSA adsorption (Figure 4).

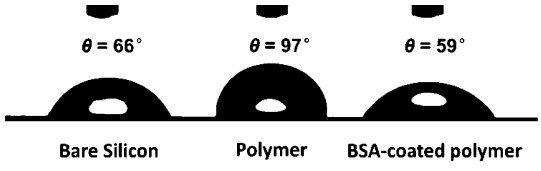

Figure 4. Static water contact angle of sol–gel polymer- and protein-coated substrate.

3.3. Protein Adsorption on the Surface of Sol–Gel Polymer. Proteins can be adsorbed on surfaces via intermolecular forces, mainly ionic bonds, hydrophobic interactions and polar interactions. Which intermolecular force exactly takes part in the interaction primarily depends on the physicochemical properties of particular surface involved. Polystyrene is generally used as ELISA plates for protein coating, taking advantage of hydrophobic amino acid residues of proteins (e.g., phenylalanine, tyrosine, leucine), which tend to retain on the hydrophobic surface of polystyrene materials. Here, benzyl group has been introduced to sol–gel to adjust the hydrophobicity of the polymer surface. Hydrophobic surface of the polymer is expected to provide a necessary binding strength, which facilitates stable attachment between material surface and a majority of proteins. At the same time, its hydrophobicity should not be so high as to essentially affect the conformation and function of the retained proteins. To evaluate the protein adsorption performance of the polymer material, three model proteins, varying in molecule size and isoelectric point (see Table S1 in the Supporting Information), had been employed to assess their retention behavior on the sol–gel polymer. BSA-FITC, IgG-FITC, and Lys-FITC conjugate solutions were incubated with the polymer at room temperature. Fluorescence micrographs were taken under identical conditions and the fluorescence intensity of these images was analyzed quantitatively (Figure 5). Further normalization

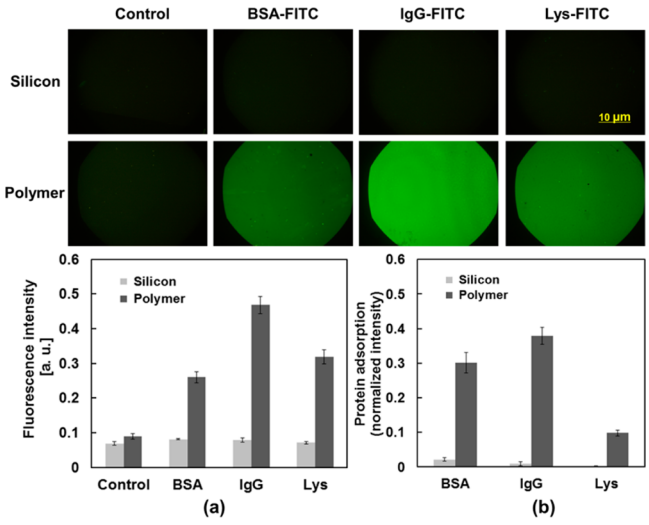

Figure 5. Protein adsorption on the surface of bare silicon slides and polymer slides Bare silicon slides (upper row) and polymer slides (lower row) were treated with PBS, BSA-FITC, IgG-FITC, and Lys-FITC conjugate solutions (from left to right). All fluorescence micrographs were taken under identical conditions: magnification 100×, exposure time 1/7 s. The fluorescence intensity of each image was (a) analyzed quantitatively and (b) normalized by removing the effect of fluorescence background and considering the individual F/P mass ratio of each protein, which allow a direct comparison of coupling amount between different proteins.

process by removing the effect of fluorescence background and taking the individual F/P mass ratio of each protein into account allow a direct comparison of coupling amount among different proteins (Figure 5b). The results showed that after incubation and intensive washing with PBS (pH7.4), all the three proteins could be effectively coated on the surface of sol–gel polymer, with green fluorescence being homogeneously distributed on the surface of each polymer substrate. It can also be observed that, with identical treatment conditions, protein adsorption on the surface of bare silicon substrates was ignorable. Of the three proteins, IgG had been observed to retain on the polymer surface with the largest amount, and Lys the smallest. This difference in binding amount might be due to the difference in molecule size of each protein. Generally, larger proteins typically bind stronger to the surface because of a larger contact area.[17] In addition, protein adsorption on a hydrophobic surface normally expresses a manner of monolayer saturation. Thus, compared to the proteins with smaller molecule weight, the larger ones (generally also having larger

dx.doi.org/10.1021/am3024355 | ACS Appl. Mater. Interfaces 2013, 5, 386–394

molecule size) would result in relatively thicker molecule layer as well as a larger binding amount.

Weak attachment has been reported as a drawback of physical immobilization, since proteins may be removed by some buffers when performing the assays.[31] Protein adsorption on the surface of sol−gel polymer was performed with a range of solution conditions to estimate the effect of pH and ionic strength on the protein immobilization (see Figure 6). The

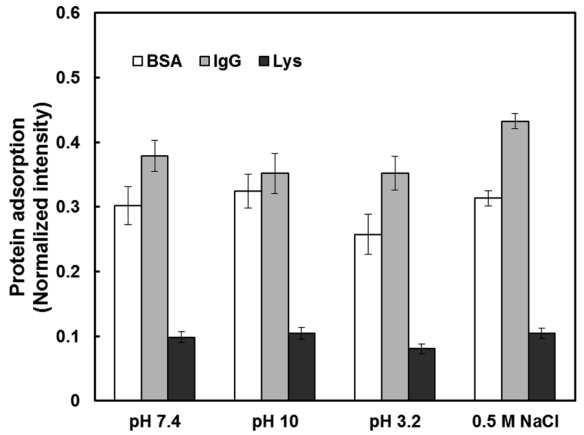

Figure 6. Effect of solution condition on the adsorption of proteins on the surface of sol−gel polymer. Solution conditions: from left to right, 0.02 M PBS, pH 7.4, containing 0.154 M NaCl; 0.1 M carbonate buffer, pH 10; 0.1 M citrate buffer, pH 3.2; 0.02 M PBS, pH 7.4, containing 0.5 M NaCl.

results showed that the effect of solution pH was limited. The three model proteins have different in isoelectric point, ranging from 4.6 to 11.1. They would exhibit various superficial charge characters at different solution conditions. For all the three proteins, no significant difference in protein binding capacities was observed for acid environment (0.1 M citrate buffer, pH 2.3) or base environment (0.1 M carbonate buffer, pH 10), compared to that obtained from a neutral binding condition (0.02 M PBS, pH 7.4). The results indicated that ionic interaction between protein and polymer surface could be negligible, which would not affect the protein binding capacity of the polymer. In the case of the current sol−gel polymer, proteins are designed to be adsorbed mainly through hydrophobic interaction. There was an evidence of binding promotion effect for IgG with the increasing of the salt concentration. When extra 0.5 M NaCl was added to the PBS solution (pH 7.4), IgG binding amount had been increased by 14.2% compared to that in a solution with physiological ion strength. In general, the sol−gel polymer has been observed to absorb proteins stably, with the protein layer well-attached within a broad range of pH and ionic strength. Such feature allows a less demanding pretreatment process before the sample to be loaded, which is especially beneficial for online analysis.

3.4. Selective Adsorption of IgG on PA-Coated Sol−gel Polymer. Whether the attached protein retains its biological activity is essential for the evaluation of a protein attachment strategy. In some cases, immobilization may lead to partial or complete loss of protein activity, due to structural deformation. *Staphylococcal* Protein A (PA) was employed in this study to investigate the influence of immobilization process on its biological activity. PA has a specific high affinity to IgG and a considerable stability over a wide range of temperatures and pH, even in the presence of denaturing agents. It has therefore been employed as a simple biochemical model for the development of an integrated optical immunosensors.[32] Because the specific adsorption of IgG depends directly on the surface coverage by biologically active PA molecules, we

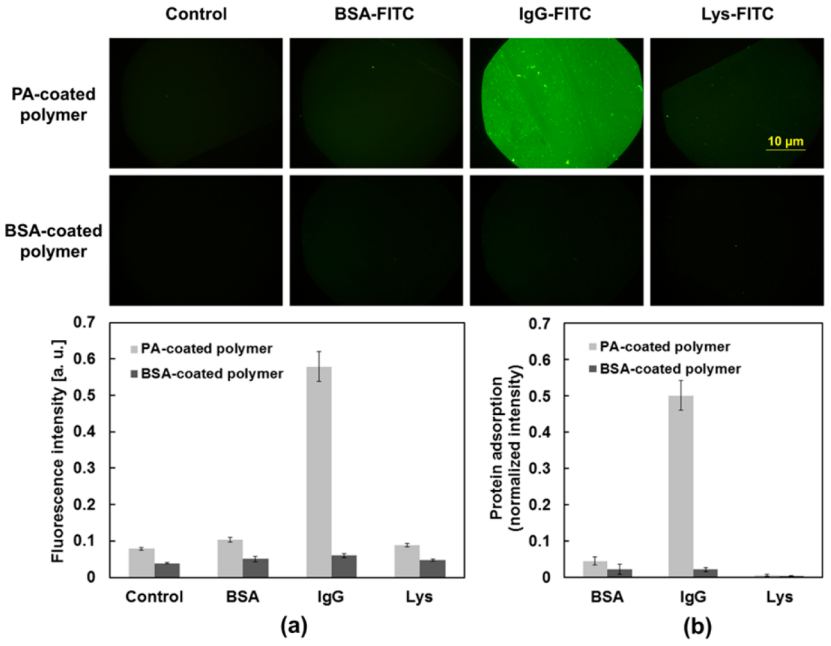

Figure 7. Selective adsorption of IgG on PA-coated polymer surface PA-coated polymer slides (upper row) and BSA-coated polymer slides (lower row) were incubated with PBS, BSA-FITC, IgG-FITC, and Lys-FITC conjugate solutions (from left to right) for 10 min at room temperature. All fluorescence micrographs were taken under identical conditions: magnification 100×, exposure time 1/7 s. The fluorescence intensity of each image was (a) quantitatively analyzed and (b) normalized by removing the effect of fluorescence background and considering the individual F/P mass ratio of each protein, which allow a direct comparison of coupling amount between different proteins.

dx.doi.org/10.1021/am3024355 | ACS Appl. Mater. Interfaces 2013, 5, 386−394

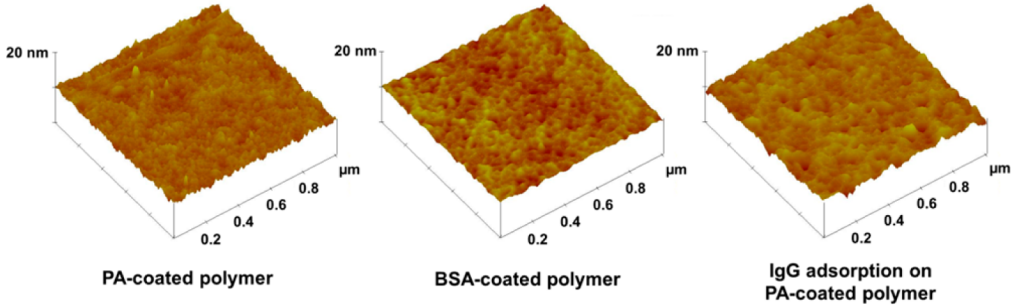

Figure 8. AFM topographical images of polymer surface with deposited proteins.

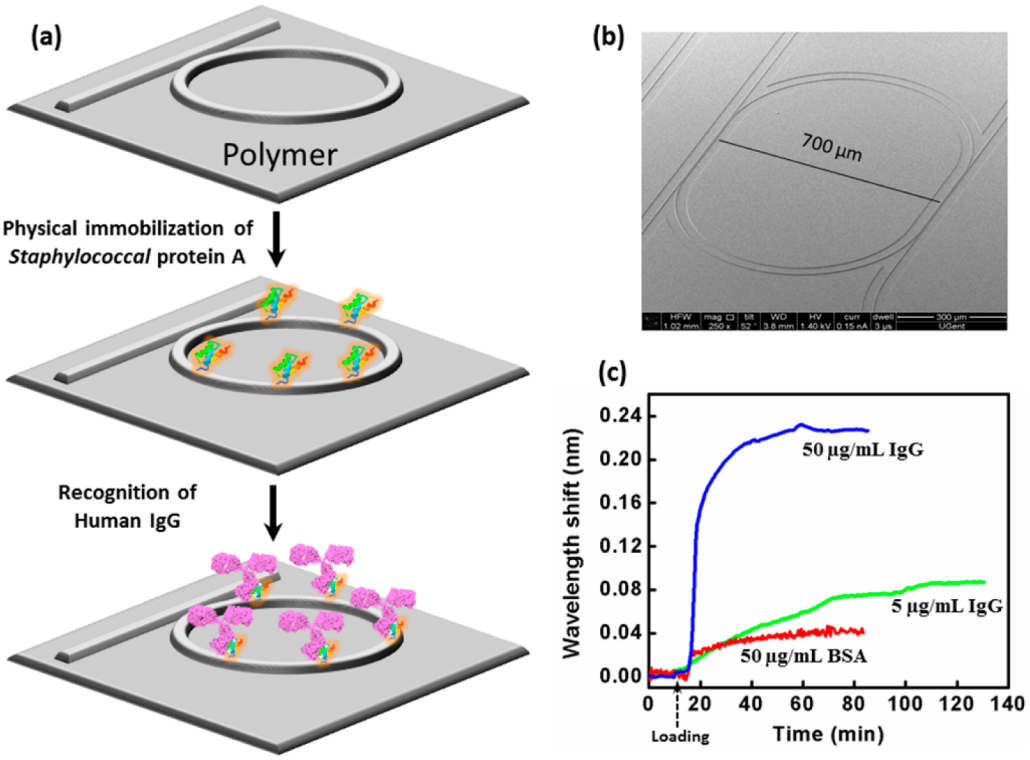

Figure 9. Biosensing using sol–gel polymer-based material platform: (a) schematic of the biosensing process using PA/IgG affinity couple; (b) SEM pictures of the ring resonator fabricated by UV-based soft imprint lithography technique; (c) response signals of the PA-coated polymer sensors to specific and nonspecific interactions. Wavelength shift obtained due to the interaction with human IgG (50 and 5 μg/mL) and with BSA (50 μg/mL). Every curve corresponds to a different experiment on a different chip. The time point of the loading of protein samples is shown in the figure.

studied the adhesion behaviors of IgG and two other control proteins, BSA and Lys, on PA-coated polymer surface to check its biological activity. PA-coated polymer slides were incubated with the three fluorescently labeled proteins at room temperature (Figure 7). After intensive rinse with PBS solution (pH 7.4) to get rid of the nonspecific adsorption of proteins, only the slide incubated with IgG-FITC showed a striking green fluorescence, indicating the binding event of IgG on the PA-coated polymer slide. The adsorption of BSA-FITC and Lys-FITC on the same slides was limited. The results indicated that the immobilization process of PA did not lead to significant loss of IgG-binding activity. More importantly, because PA has a relatively small molecular size and a less complex spatial structure, the surface of the polymer had a good coverage by the protein layer and therefore reached saturation. Thus, the surface area that could accommodate other proteins, which would result in nonselective adsorption, was limited. As a control, BSA-coated polymer slides were also employed and incubated with the three proteins under the same conditions. No significant adsorption of the all three model proteins had been observed on BSA-coated polymer slides, indicating the formation of dense BSA layer on the polymer surface. Accordingly, for the current polymer platform, BSA could also perform as an efficient blocking protein to take up the residual binding sites in order to prevent the nonspecific binding of unwanted proteins.

Topographical diversity of polymer surface could be also observed for different protein layers (Figure 8). After PA was deposited on the polymer slide from a water solution with 2 mg/mL of PA for 1h, the AFM topographical image (Figure 8, left) clearly displayed a densely packed two-dimensional protein film covering a flat polymer surface, indicating that the adsorption had reached saturation. Dense and homogeneous protein layer of BSA could be also obtained (Figure 8, middle). Similar to what has been observed previously by Coen.[33] It was found that deposited PA molecules were

dx.doi.org/10.1021/am3024355 | ACS Appl. Mater. Interfaces 2013, 5, 386–394

uniformly distributed over the surface with each protrusion shape occupying a disc of 3−4 nm in diameter. The height of the proteins lay between 2 and 3 nm. Taking into account that the mean size of PA in solution is 3 nm, the dimension of the deposited PA was therefore equal with its natural size in solution, which constitutes a favorable sign for nondenaturation of PA. After IgG was adsorbed on PA-coated polymer, AFM topographical images showed a significant change in surface morphology (Figure 8, right). The adsorption of IgG induced a remarkable increase in surface roughness, with the Rms increasing from 0.538 to 0.756 nm. The IgG molecules were distributed over the whole surface and form cauliflower aggregates of 10 to 70 nm in diameter. You and Lowe[34] reported a methodology to differentiate nonspecifically or specifically adsorbed IgG by AFM pictures; they found that the specifically adsorbed IgG through PA always present a granular structure, similar to what we observed in this study. The height difference between holes and aggregates comprises between 8 and 13.5 nm, which had been considered to correspond to the height of an IgG (8.5 nm) or an IgG on top of one or two protein A (11.5−14.5 nm). Therefore, the AFM feature of an IgG that is specifically bonded to protein A by the Fc end corresponds to two height maxima separated by 14 nm.[33] According to this estimate, several features of this kind can be detected on the picture (Figure 8, right). Taking into account that the IgG hinges between the Fab and Fc segments are highly flexible structures, we can affirm that these structures represent standing up IgG.

3.5. Optical Biosensing Experiments of Specific and Nonspecific Interactions. PA/IgG affinity couple has been used as an affinity model to demonstrate the biosensing process of polymer resonators. Treatments of the microring resonator biosensor are schematically pictured in Figure 9a. Sol−gel polymer based ring resonator chips were fabricated using UV-soft imprint technique, with the diameter of the microrings being 700 μm (Figure 9b). Entire sensing processes were monitored and shown in Figure 9c. Through a fluidic channel, PA-coated polymer chip was rinsed with DI (deionized) water and PBS solution (0.01M, pH 7.4), and then loaded with IgG at a concentration of 50 μg/mL in PBS. An abrupt increase of resonant wavelength was detected at the early stage of IgG loading, indicating the fast surface binding of IgG molecules to the immobilized PA layer. When the sensor surface reached saturation, PBS was pumped into the system to rinse the surfaces of the polymer ring resonator. At this stage, no obvious reverse wavelength shift was observed during PBS rinsing, which indicates the strong binding between PA and IgG. It is also a proof that coating of PA to the chip surface is successful, in terms of stable immobilization of PA on the polymer surface as well as good maintaining of its biological activity. In consist with the performance reported for silicon-based chips,[13] PA-coated polymer sensors exhibited different dynamic responsivitis toward the samples of different IgG concentration. For the low concentration, a slow wavelength shift was recorded due to the slow transport of the molecules to the surface. So far, the human IgG with the concentration down to 5 μg/mL can be easily detected with the signal recorded as 90 pm (Figure 9c), which exceeds the noise level for about 45 times.

The nonspecific binding is another important aspect for the label-free optical biosensor. To test our polymer-based optical biosensor's response toward nontargeted biomolecules, we chose BSA as a control protein and brought into contact with the PA-coated microring surface. The concentration of the BSA for the test was 50 μg/mL (in 0.01 M PBS, pH 7.4). As can be seen, there was a resonant wavelength shift of around 40 pm caused by the nonspecific binding of the BSA molecules, where the saturation was reached after 40 min with the injection of the BSA solution. Besides that, there was no apparent signal change after the PBS flowed over the optical biosensor, which indicated that the BSA molecules were absorbed onto the surface of biosensor and could not be washed away by PBS. In spite of the presence of BSA adsorption, the resonant wavelength shift of 40 pm caused by 50 μg/mL of BSA is still smaller than that of 90 pm by specific binding of the human IgG with a concentration of 5 μg/mL (see Figure 9c), validating the recognition ability of the PA-coated microring sensors. Actually, similar extent of BSA nonspecific adsorption was also reported for a silicon-based platform, and this situation was much improved by introducing PEG chemistry.[13] Further improvement of the current polymer biosensing platform can be more straightforward. In fact, following the PA-coating process, a blocking step using BSA (or other blocking molecules used in ELISA) can be helpful to take up the residual binding sites on the sensor surface, which is expected to be a potential method to reduce the nonspecific binding of unwanted proteins during the subsequent surface sensing process.

4. CONCLUSION

We have utilized a sol−gel system to fabricate microring resonator biosensors. This type of polymer-based material system is able to play the double roles of both optical waveguide and favorable carrier for noncovalent immobilization of proteins, so that the biosensor device is free from any additional step of surface modification to bind receptor molecules. For the current material platform, optical microrings with desired surface characteristics, in terms of modest hydrophobicity and controlled roughness, can be readily fabricated. Monolayers of receptor proteins can be formed by simply immersing the waveguide surface in a solution of the proteins. The immobilized proteins showed a dense coverage onto the surface of waveguide, with their biological activities maintained well. This study confirmed the potential of preparing dense, homogeneous, specific, and stable biosensing surfaces by immobilizing receptor proteins on polymer sensor through direct physical attachment. This will facilitate both the fabrication and use of sensor devices, thus provides a novel strategy for the development of robust and cost-effective optical biosensors. It is expected that such polymer waveguide could be of especial interest for the development of optical biosensing platform for multidimensional arrays.

■ ASSOCIATED CONTENT

Ⓢ Supporting Information

Graphic description of the basic principle of a microring resonator biosensor (Figure S1), and detailed preparation processes of fluorescently labeled proteins and their properties (Figure S2 and Table S1). This material is available free of charge via the Internet at http://pubs.acs.org/.

■ AUTHOR INFORMATION

Corresponding Author

*Tel.: (86) 411 84706125. Fax: (86) 411 84706125. E-mail: mszhao@dlut.edu.cn (M.S.Z.); lyj81@dlut.edu.cn (L.Y.J.).

Notes

The authors declare no competing financial interest.

■ ACKNOWLEDGMENTS

This work was supported by the National Natural Science Foundation of China (21204009 and 61077015), National High-tech R&D Program (2012AA040406), Natural Science Foundation of Liaoning Province (20102020) and Fundamental Research Funds for the Central Universities (DUT13JB01 and DUT12RC(3)05). The authors thank Dr. Fang Cheng (School of Pharmaceutical Science and Technology, Dalian University of Technology) for helpful suggestions.

■ REFERENCES

(1) Chandra, H.; Reddy, P. J.; Srivastava, S. *Expert Rev. Proteomics* **2011**, *8*, 61−79.
(2) Villiers, M. B.; Cortès, S.; Brakha, C.; Lavergne, J. P.; Marquette, C. A.; Deny, P.; Livache, T.; Marche, P. N. *Biosens. Bioelectron.* **2010**, *26*, 1554−1559.
(3) Chang, T. Y.; Huang, M.; Yanik, A. A.; Tsai, H. Y.; Shi, P.; Aksu, S.; Yanik, M. F.; Altug, H. *Lab Chip* **2011**, *11*, 3596−3602.
(4) Ramachandran, A.; Wang, S.; Clarke, J.; Ja, S. J.; Goad, D.; Wald, L.; Flood, E. M.; Knobbe, E.; Hryniewicz, J. V.; Chu, S. T.; Gill, D.; Chen, W.; King, O.; Little, B. E. *Biosens. Bioelectron.* **2008**, *23*, 939−944.
(5) Luchansky, M. S.; Bailey, R. C. *Anal. Chem.* **2012**, *84*, 793−821.
(6) Scheler, O.; Kindt, J. T.; Qavi, A. J.; Kaplinski, L.; Glynn, B.; Barry, T.; Kurg, A.; Bailey, R. C. *Biosens. Bioelectron.* **2012**, *36*, 56−61.
(7) Luchansky, M. S.; Bailey, R. C. *Anal. Chem.* **2010**, *82*, 1975−1981.
(8) Luchansky, M. S.; Bailey, R. C. *J. Am. Chem. Soc.* **2011**, *133*, 20500−20506.
(9) Washburn, A. L.; Gunn, L. C.; Bailey, R. C. *Anal. Chem.* **2009**, *81*, 9499−9506.
(10) Wang, S.; Ramachandran, A.; Ja, S. J. *Biosens. Bioelectron.* **2009**, *24*, 3061−3066.
(11) Chao, C.; Fung, W.; Guo, L. *IEEE J. Sel. Top. Quantum Electron.* **2006**, *12*, 134−142.
(12) Ksendzov, A.; Lin, Y. *Opt. Lett.* **2005**, *30*, 3344−3346.
(13) De Vos, K.; Girones, J.; Popelka, S.; Schacht, E.; Baets, R.; Bienstman, P. *Biosens. Bioelectron.* **2009**, *24*, 2528−2533.
(14) Shang, J.; Cheng, F.; Dubey, M.; Kaplan, J. M.; Rawal, M.; Jiang, X.; Newburg, D. S.; Sullivan, P. A.; Andrade, R. B.; Ratner, D. M. *Langmuir* **2012**, *28*, 3338−3344.
(15) Byeon, J. Y.; Limpoco, F. T.; Bailey, R. C. *Langmuir* **2010**, *26*, 15430−15435.
(16) Hanefeld, U.; Gardossi, L.; Magner, E. *Chem. Soc. Rev.* **2009**, *38*, 453−468.
(17) Rabe, M.; Verdes, D.; Seeger, S. *Adv. Colloid Interface Sci.* **2011**, *162*, 87−106.
(18) Mücksch, C.; Urbassek, H. M. *Langmuir* **2011**, *27*, 12938−12943.
(19) Hartvig, R. A.; van de Weert, M.; Ostergaard, J.; Jorgensen, L.; Jensen, H. *Langmuir* **2011**, *27*, 2634−2643.
(20) Qian, W.; Yao, D.; Yu, F.; Xu, B.; Zhou, R.; Bao, X.; Lu, Z. *Clin. Chem.* **2000**, *46*, 1456−1463.
(21) Zhang, Y.; Zhang, J.; Huang, X.; Zhou, X.; Wu, H.; Guo, S. *Small* **2012**, *8*, 154−159.
(22) He, C.; Liu, J.; Xie, L.; Zhang, Q.; Li, C.; Gui, D.; Zhang, G.; Wu, C. *Langmuir* **2009**, *25*, 13456−13460.
(23) Chen, B.; Miller, E. M.; Miller, L.; Maikner, J. J.; Gross, R. A. *Langmuir* **2007**, *23*, 1381−1387.
(24) Deng, T.; Wang, J.; Liu, Y.; Ma, M. *J. Appl. Polym. Sci.* **2010**, *115*, 1168−1175.
(25) Abrol, K.; Qazi, G. N.; Ghosh, A. K. *J. Biotechnol.* **2007**, *128*, 838−848.
(26) Brynda, E.; Pacherník, J.; Houska, M.; Pientka, Z.; Dvorák, P. *Langmuir* **2005**, *21*, 7877−7883.
(27) Zhang, J.; Wang, J.; Wang, L.; Han, X.; Zhao, M.; Jian, X. *J. Sol-Gel Sci. Technol.* **2010**, *56*, 197−202.
(28) Zhang, H.; Wang, J.; Li, L.; Song, Y.; Zhao, M.; Jian, X. *J. Macromol. Sci., Part A: Pure Appl.Chem.* **2008**, *45*, 232−237.
(29) Teng, J.; Scheerlinck, S.; Zhang, H.; Jian, X.; Morthier, G.; Beats., R.; Han, X.; Zhao, M. *IEEE Photonics Technol. Lett.* **2009**, *21*, 1323−1325.
(30) Johnson, B. N.; Mutharasan, R. *Langmuir* **2012**, *28*, 6928−6934.
(31) Rusmini, F.; Zhong, Z.; Feijen, J. *Biomacromolecules* **2007**, *8*, 1775−1789.
(32) Mun, K. S.; Alvarez, S. D.; Choi, W. Y.; Sailor, M. J. *ACS Nano* **2010**, *4*, 2070−2076.
(33) Coen, M. C.; Lehmann, R.; Gröning, P.; Bielmann, M.; Galli, C.; Schlapbach, L. *J. Colloid Interface Sci.* **2001**, *233*, 180−189.
(34) You, H. X.; Lowe, C. R. *J. Colloid Interface Sci.* **1996**, *182*, 586−601.